Low-temperature conversion of Fe-rich sludge to KFeS₂ whisker: a new flocculant synthesis from laboratory scale to pilot scale

Dongxu Liang[1], Yu Chen[1], Suiyi Zhu[1*], Yidi Gao[1], Tong Sun[1], Kyonghun Ri[1,2] and Xinfeng Xie[3]

Abstract

Herein, a KFeS₂ whisker was formed in mass production at a low temperature, with waste cold-rolling sludge as Fe source, which exhibited good performance in the removal of Zn/Ni from real electroplating effluent. At laboratory scale, KFeS₂ was generated at 80 °C by the hydrothermal method, and KFeS₂ whisker grew radially with the extension of the reaction time. This method was applied at pilot scale, where a similar KFeS₂ whisker was also produced with waste cold-rolling sludge as Fe source, and a residual brownish supernatant was observed after the reaction and then completely recycled in the next round for KFeS₂ synthesis. After recycling five times, the produced KFeS₂ whisker did not change. The drying and storage of KFeS₂ have also been verified. Freeze drying and vacuum drying were applicable, whereas air drying was not profitable. Moreover, the efficiency of Zn/Ni removal using undried KFeS₂ was similar to that of dried KFeS₂. The efficiencies of Zn/Ni removal using KFeS₂ were apparently higher those of common reagents for wastewater treatment.

Keywords: KFeS₂ whisker, Low-temperature hydrothermal conversion, Pilot scale, Treatment of electroplating effluent

Introduction

KFeS₂ is a fibrous Fe/S-bearing mineral [1] crystallised under high potassium activity and sulphur fugacity [2]. Such conditions are extreme; thus, KFeS₂ has not been detected in natural rocks. However, its derivate, rasvumite, co-exists with pegmatites in the mafic environment [3]. KFeS₂ is usually synthesised artificially, and it has a special structure, in which one Fe atom is covalent with four sulphur atoms to form a stable tetrahedral $(FeS_2)_n^{n-}$ bond [4]. The free electrons in large spaces located at edge-sharing $(FeS_2)^{2-}$ chains are neutralised by K⁺ [5] to form a stable Fe-S structure. In the synthesis of KFeS₂, when cations, such as Ag⁺, Ca²⁺, Sr²⁺ and Ba²⁺, are introduced [6,

7], they will be embedded into the inner lattice via the space channel of $(FeS_2)^{2-}$ [6], and K⁺ is released and escapes, resulting in the replacement reaction between cations and K⁺. Thus, KFeS₂ is an important raw material [8, 9] to produce new ternary metal thioferrate products, including RbFeS₂ [10, 11], AgFeS₂ [7, 12] and CuFeS₂ [12]. Such products are essential photovoltaic materials [13, 14] and a photothermal platform for medical therapy [15, 16], thereby increasing the demand for KFeS₂.

In the early research, the solid burning method was widely used in the synthesis of KFeS₂. For the solid-phase reaction, iron, as a raw material, was mixed with sulphur and K source (e.g., K₂CO₃ and K₂S₂) [10, 17] and then burned in a reducing atmosphere [18]. During cauterisation, the oxidation of iron and sulphur occurred, followed by solid conversion to form a $(FeS_2)^{2-}$ structure; K⁺ was located at edge-sharing $(FeS_2)^{2-}$ chains

* Correspondence: papermanuscript@126.com
[1]Science and Technology Innovation Center for Municipal Wastewater Treatment and Water Quality Protection, Northeast Normal University, Changchun 130117, China
Full list of author information is available at the end of the article

to form $KFeS_2$ needle-shaped crystals. For instance, Bronger et al. [18] prepared $KFeS_2$ samples by reacting K_2CO_3 with iron under a H_2S atmosphere at 1000 K for 6 h. After extraction with water and alcohol, well-developed needle-shaped violet $KFeS_2$ crystals were generated. The burning method consumes considerable energy to maintain a high temperature, and it has strict requirements on the reaction system such as a reducing atmosphere, which leads to high costs. Thus, $KFeS_2$ cannot be produced on a large scale. Compared with the burning method, the solvothermal method shows a clear advantage in lowering the reaction temperature. Han et al. [9] mixed KNO_3, Fe $(NO_3)_3 \cdot 9H_2O$ and S powder in ethylenediamine solution; after heating at 190 °C for 18 h, a black $KFeS_2$ powder was obtained. However, in the presence of deionised water, Fe_2O_3 was predominant in the product [9]. The extensive use and consumption of organic solvents limit their production on a large scale. To date, a more economical method of mass production of $KFeS_2$ remains unknown.

For mass production of $KFeS_2$, reducing the costs is necessary. The high cost of $KFeS_2$ synthesis is primarily due to the chemical reagents used in the raw materials and high temperature. Firstly, weakly crystalline iron compounds can dissolve and release Fe $(OH)_4^-$ [19] in alkaline solutions, which is the intermediate product before HS^- substitution reaction in the synthesis of $KFeS_2$. Therefore, the cost of raw materials can be reduced by replacing chemically pure iron sources with iron-containing wastes. Herein, cold-rolling sludge, which was precipitated from Fe-bearing picking wastewater by adjusting the wastewater to pH 8 in a weakly crystallised form, was used as a raw material to explore the potential application of Fe-rich sludge as an Fe source to synthesise $KFeS_2$. Secondly, the solvothermal method can reduce the synthesis temperature compared with the sintering method, but it will consume a large amount of organic solvents and increase the synthesis cost of $KFeS_2$. In the previous study, it was found that $KFeS_2$ can be synthesised in KOH solution at 160 °C. However, Han et al. reported that Fe_2O_3 was generated simultaneously [9]. Therefore, the synthesis of $KFeS_2$ using the hydrothermal method whilst suppressing the formation of Fe_2O_3 must be developed. According to the research of hydrothermal synthesis of Fe_2O_3, the reaction temperature is between 100 and 200 °C [20–25]. This finding shows that high temperature is conducive to the formation of Fe_2O_3, and reducing the temperature may avoid the formation of Fe_2O_3. Therefore, a method of lowering the reaction temperature to reduce the cost and avoid the formation of Fe_2O_3 is necessary. Thirdly, given the high potassium activity and sulphur fugacity for the formation conduction of $KFeS_2$ [2], the supernatant was rich in K^+ and HS^-, and it has high alkalinity

after $KFeS_2$ synthesis reaction. If the supernatant could be recycled for the next synthesis reaction, then the synthesis cost will be greatly reduced. Finally, the drying and storage methods of $KFeS_2$ must also be considered from the perspective of cost reduction.

In neutral or weakly alkaline solution, the skeleton structure of $KFeS_2$ hydrolysis is spontaneous, and the decomposition of $(FeS_2)_n^{n-}$ generates several Fe/S-bearing flocs [26]. Such Fe/S-bearing flocs are rich in Fe-SH and Fe-OH groups, which show good affinity for heavy metals in solution [27]. The behaviour of $KFeS_2$ decomposition is similar to the common flocculants, namely, poly aluminium chloride and polymeric ferric sulfuric. However, no reports have been found on $KFeS_2$ applied in wastewater treatment. Electroplating wastewater contains significant quantities of heavy metals, organic compounds and surfactants [28–30], which is considered a hazardous source. Given the use of plating additives, heavy metals are complexed with organics to form stable organic-heavy metal ligands [31–34]. Thus, they are refractory to be removed, although the precipitates (e.g., lime and polymeric ferric sulfuric) are added. Thus, electroplating wastewater is used as a pollutant to verify the performance of $KFeS_2$ in wastewater treatment.

Here, the pilot-scale conversion of waste Fe-rich sludge to $KFeS_2$ was successfully implemented at a low temperature and atmospheric pressure. The upcycling of supernatant in the synthesis of $KFeS_2$ was explored. The storage of prepared $KFeS_2$ was also optimised in the range of freeze drying, vacuum drying, air drying and wet storage. The produced $KFeS_2$ showed superior efficiencies in the removal of Zn/Ni from real electroplating effluent.

Materials and methods
Material
Ferric nitrate nonahydrate (Fe $(NO_3)_3 \cdot 9H_2O$, AR) was purchased from Tianjin Yongsheng Fine Chemical Co. Potassium sulphide (K_2S, AR) was purchased from Aladdin Co. Potassium hydroxide (KOH, AR) was purchased from Tianjin Hengxing Chemical Reagent Manufacturing Co. Ferrihydrite-bearing sludge (known as sludge) was collected from the sludge warehouse of Guixi Cold-rolling Company (Changchun, China). The sludge contained 41.2% Fe, 50.5% water content and less than 10% carbon. Deionised water was used as experimental water in all lab-scale experiments. In pilot scale, tap water was used.

Laboratory-scale experiment for $KFeS_2$ whisker synthesis
In laboratory-scale experiments, ferrihydrite was synthesised by adding 40 g of Fe $(NO_3)_3 \cdot 9H_2O$ to 500 mL of deionised water and then mixed with 330 mL of 1 M KOH under stirring at 120 rpm. After 1 h, a mixed solution was generated and placed on the laboratory bench for another

2 h. A brownish sediment was produced at the bottom of the solution, which was collected and washed with deionised three times. The sediment (known as Ferr) was air dried at 60 °C for subsequent use.

The laboratory-scale conversion of Ferr to $KFeS_2$ whisker was performed as follows. Firstly, 1 g of Ferr, 3.3078 g of K_2S and 30 mL of 6 M KOH solution were mixed in a 50 mL beaker. Secondly, the beaker was sealed with parafilm and then magnetically stirred at 200 rpm at 50 °C. Thirdly, after 10 h, the beaker was cooled to room temperature and placed at a table for another 2 h. Fourthly, a black deposit was formed at the base of the beaker, which was collected and freeze dried at −80 °C for 24 h. The dried product was named as E50−10, where E represents the experimental-scale synthesis; 50 is the heating temperature, and 10 is the heating time.

The effect of heating temperature was investigated by changing the heating temperature from 50 to 80 °C following the above-mentioned steps. Then, the corresponding product was named as E80−10. A control experiment was also performed following the above-mentioned steps, where the heating time was extended from 10 h to 24 h, and the products were named as E50−24 and E80−24.

Pilot-scale production of $KFeS_2$ whisker

A pilot-scale vessel was made to synthesise $KFeS_2$ whisker at mass production (Fig. 1). In step 1, sludge (0.3 kg), K_2S (1.10 kg) and KOH (3.36 kg) with a molar ratio of Fe: K_2S: KOH = 1:5:30 and 10 L of tap water were added to a bucket with a volume of 15 L under stirring at 120 rpm for 1 h to generate a black suspension. In step 2, the suspension was transferred into a sealed vessel and then heated at 80 °C for 24 h. In step 3, the solid sediment and suspension in the vessel were transferred into the suction filter. After filtration, the solid fraction and filter liquor were collected separately. In step 4, the solid fraction (P80−24) was stored in a bucket, in which a small portion of the solid was freeze dried at −80 °C overnight.

The supernatant generated in step 3 was recycled in the next round (Fig. 1). The total volume of supernatant was adjusted to 10 L with supplementary tap water, followed by adding 0.3 kg of sludge, 0.44 kg of K_2S and 0.11 kg of KOH under stirring at 120 rpm. After 1 h, a suspension was generated and then treated following the above-mentioned steps. The generated product was named as P80−24-1 (1 represents the recycle number of supernatant), whilst the generated supernatant was collected again for further use. The recycle experiment of the supernatant was performed four times at pilot scale, and the corresponding products were named as P80−24-2, P80−24-3, P80−24-4 and P80−24-5.

The drying method of $KFeS_2$ was also optimised. Two typical drying methods, vacuum drying at 60 °C and air
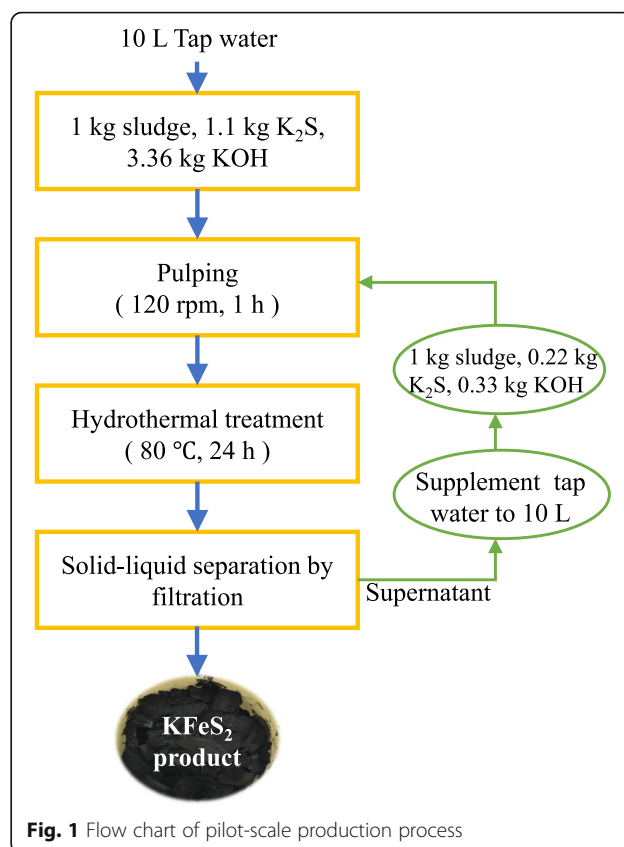

Fig. 1 Flow chart of pilot-scale production process

drying at 105 °C, were investigated using P80−24 as the targeted $KFeS_2$ product, in comparison with that of freeze drying.

Application of $KFeS_2$ whisker in real electroplating wastewater treatment

Electroplating wastewater was treated with polymeric aluminium chloride and precipitant (e.g., diethyldithiocarbamate) in the wastewater plant of Jitong Machinery Company (Changchun, China). The effluent discharge from the wastewater plant was collected and used in this study to determine the performance of the synthesised $KFeS_2$ products. The effluent contained 7.8 mg L^{-1} Zn and 0.6 mg L^{-1} Ni at pH 7.42, which was treated as follows. Approximately 0.2 g of P80−24 was mixed with 1000 mL of effluent in a 2000 mL beaker under stirring at 100 rpm for 2 h. Subsequently, the beaker was placed on the laboratory bench for 2 h to settle particles, whilst 1 mL of supernatant was sampled for characterisation. Control experiments were performed by changing the P80−24 dosage from 0.2 to 0.5, 1, 3, 5 and 10 g. Other products, including the undried P80−24, P80−10, P80−24-1 and P80−24-5, were also used to treat the effluent in accordance with the above-mentioned method and then compared with common reagents, such as $Na_2S\cdot9H_2O$, polymeric ferric sulfuric, sodium diethyldithiocarbamate and lime.

The zeta potential and hydrodynamic radius of P80–24 were also investigated. Approximately 0.1 g of P80–24 was dispersed in 100 mL of effluent under constant stirring at 150 rpm to form a mixture solution. At a given interval, 5 mL of solution was sampled and then determined by a zeta potentiometer (Nano-ZS, Malvern, UK). The experiment of P80–24 in deionised water was also performed in accordance with the above-mentioned method.

Characterisation

The morphologies of the samples were observed by scanning electron microscope (SEM, JSM-6400, Jeol, Japan), and the surface of the samples were sputter-coated with gold prior to observation. The crystallography properties of the samples were characterised by X-ray diffractometer (XRD, Rint2200, Rigaku Corporation, Japan) using Cu-Kα radiation. The valance state of surface elements of the samples was investigated by X-ray photoelectron spectroscopy (XPS, ADES-400, VG Scientific, Britain).

Results and discussion
Laboratory-scale synthesis of KFeS$_2$ whisker

The synthesis of KFeS$_2$ whisker at low temperature was optimised at lab scale. At 50 °C, the product was weakly crystallised, which showed a small rod-shaped precursor (Fig. 2 (E50–10)), although the heating time was extended from 10 to 24 h (Fig. 2 (E50–24)). By increasing the temperature from 50 to 80 °C, the product E80–10 appeared as sharp whisker particles with 0.2 μm diameter and 0.5–1 μm length, which indicated the representative peaks of KFeS$_2$ (Fig. 2 (E80–10)). After the reaction for 24 h, the product E80–24 showed that the peaks of KFeS$_2$ were sharp (Fig. 2 (E80–24)), and its whisker grew radially to 1–4 μm. This finding demonstrated that 80 °C was an optimal temperature for sharp KFeS$_2$ synthesis.

Mass production of KFeS$_2$ whisker at pilot scale

Pilot-scale synthesis of KFeS$_2$ was performed at 80 °C for 24 h, and the results are shown in Fig. 3. The sludge was an irregular block (Fig. 3A sludge) that showed typical peaks of ferrihydrite and carbon (Fig. 3B sludge). After the reaction, the product P80–24 was a well-formed whisker that showed sharp peaks of KFeS$_2$ (Fig. 3B (P80–24)), which was similar to E80–24 synthesised at lab scale (Fig. 2 (E80–24)). Although impure carbon was mixed with ferrihydrite in the sludge, the XRD peaks of carbon were not recorded after the reaction, revealing that it was covered by KFeS$_2$ whisker and was not observed by an XRD diffractometer. The above-mentioned findings indicated that mass production of KFeS$_2$ whisker was successfully achieved.

Upcycling of supernatant during KFeS$_2$ synthesis

At pilot scale, the supernatant was recycled as an alkaline solution for KFeS$_2$ synthesis in the next round, and the results are shown in Fig. 4. In the first round, the product P80–24-1 showed sharp peaks of KFeS$_2$ and well-formed whisker (Fig. 4), which was similar to that without supernatant recycling (Fig. 3 (P80–24)). After recycling for five times, typical KFeS$_2$ whisker was also observed for the product P80–24-5 (Fig. 4 (P80–24-5)), suggesting that the recycling route of supernatant was applicable for KFeS$_2$ synthesis. The supernatant was highly alkaline; recycling not only reduced KOH consumption and used sufficient HS$^-$ and S^{2-} for KFeS$_2$ synthesis but also avoided the generation of waste alkaline wastewater.

Optimisation of the drying method

The prepared P80–24 was dried in three ways, namely, freeze drying, air drying and vacuum drying. In freeze drying, the product was in the form of KFeS$_2$ whisker (Fig. 3 (P80–24)). In comparison with freeze drying, the
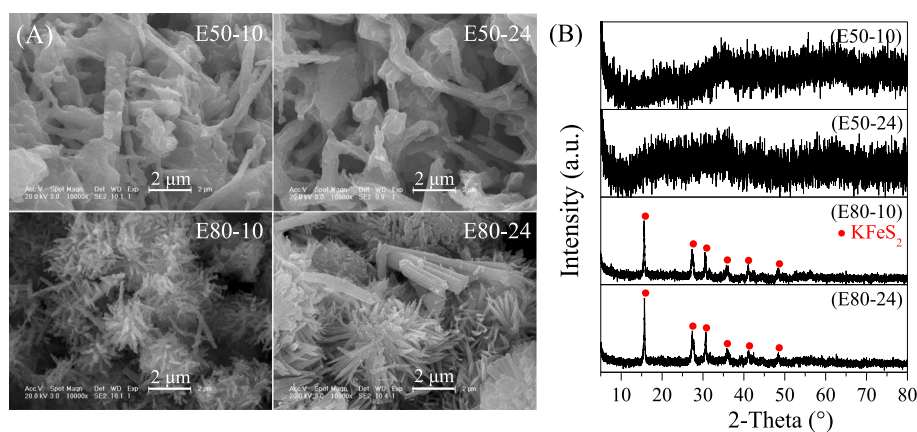

Fig. 2 (**A**) SEM photomicrographs and (**B**) XRD patterns of E50–10, E50–24, E80–10 and E80–24
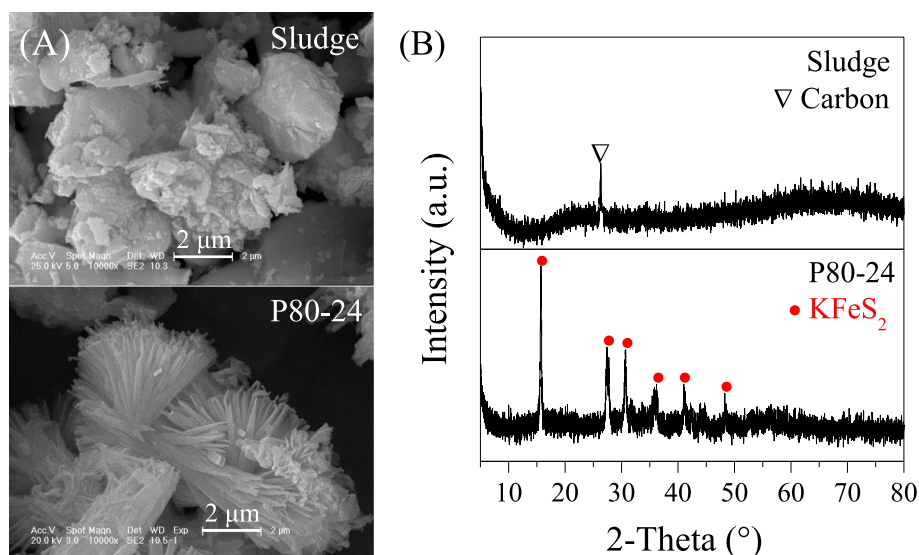
Fig. 3 (**A**) SEM photomicrographs and (**B**) XRD patterns of the sludge and product P80–24 at pilot scale

product from vacuum drying also exhibited well-formed sharp whisker and XRD pattern of $KFeS_2$, although a small portion of broccoli-shaped aggregates was recorded (Fig. 5A (vacuum drying)). Such aggregates were generated by the oxidation of structural S in $KFeS_2$ whisker. However, after air drying at 105 °C, $KFeS_2$ peaks were observed (Fig. 5B (air drying)), but abundant broccoli-shaped aggregates were generated, demonstrating that the oxidation of S was accelerated during air drying. These results demonstrated that freeze drying and vacuum drying were effective for $KFeS_2$ whisker dewatering. Wet P80–24 without dewatering was stored

in a sealed bucket for a week, dehydrated and freeze dried again to investigate the storage of $KFeS_2$ whisker. The corresponding product was also in the form of a sharp whisker with clear $KFeS_2$ peaks (Fig. S1), demonstrating that the wet storage of $KFeS_2$ was a desirable route. The wet sample of P80–24 was also used in the wastewater treatment as discussed below.

Application in raw electroplating wastewater treatment
$KFeS_2$-bearing products were used in the treatment of real electroplating effluent (Fig. 6A). The effluent had a pH of 7.42, and it contained 7.8 mg L^{-1} Zn and 0.6 mg
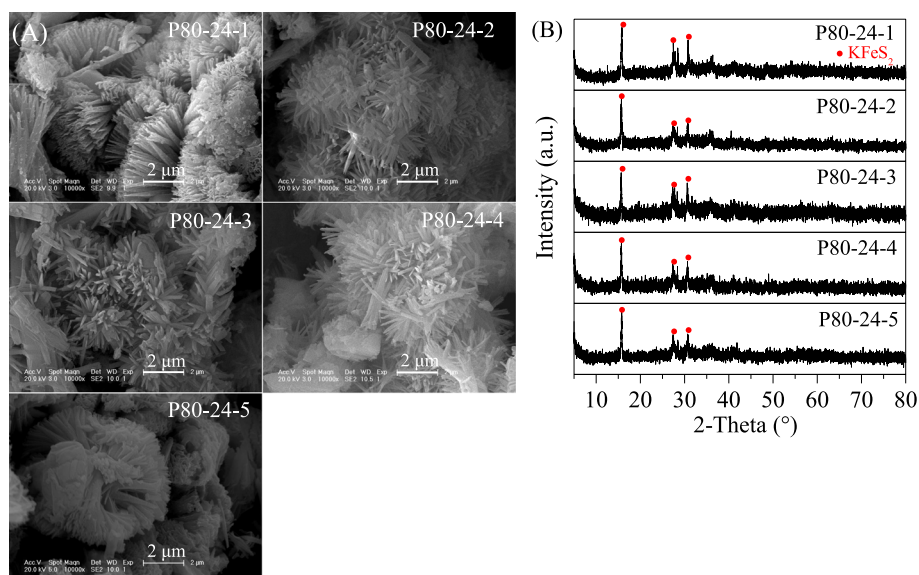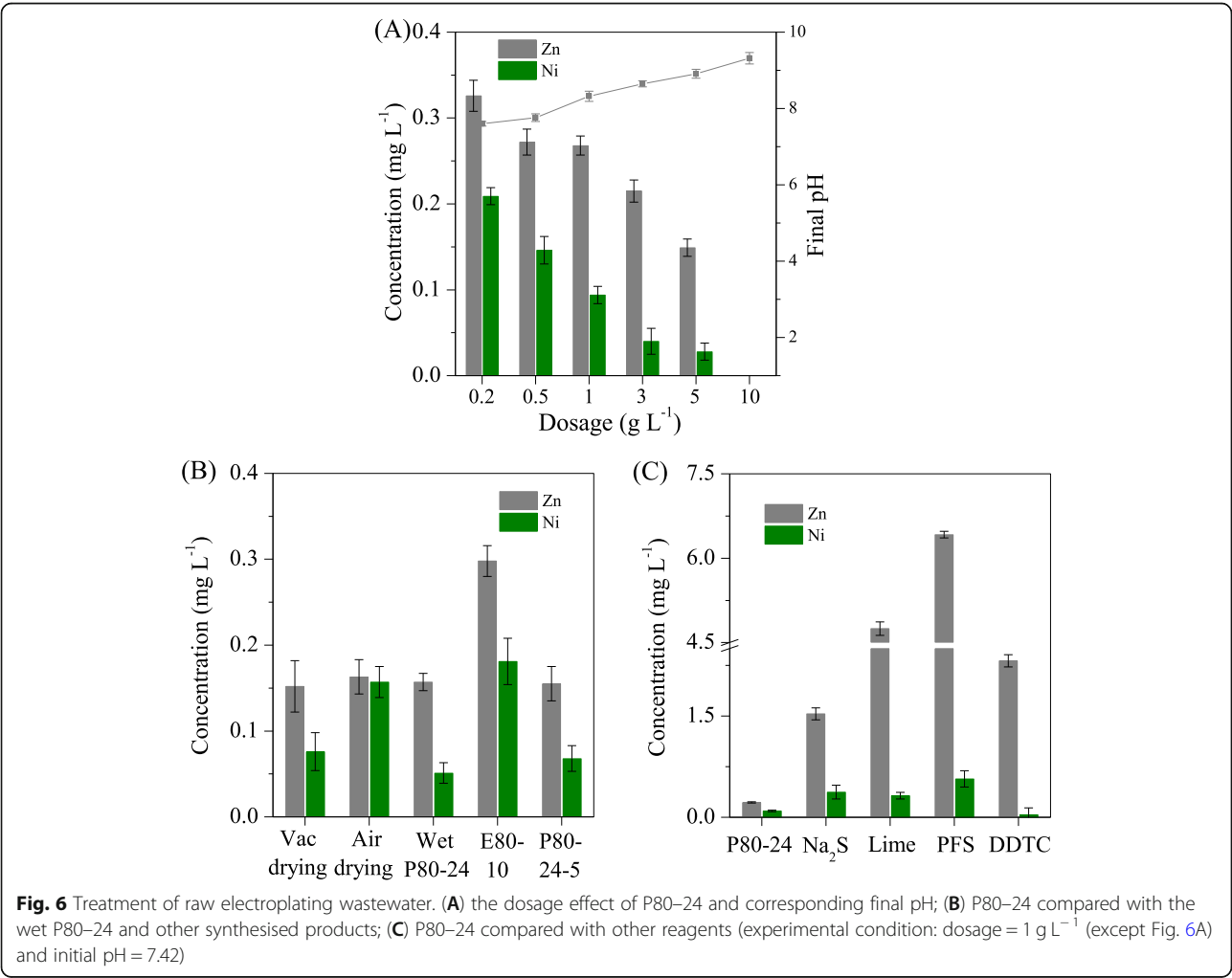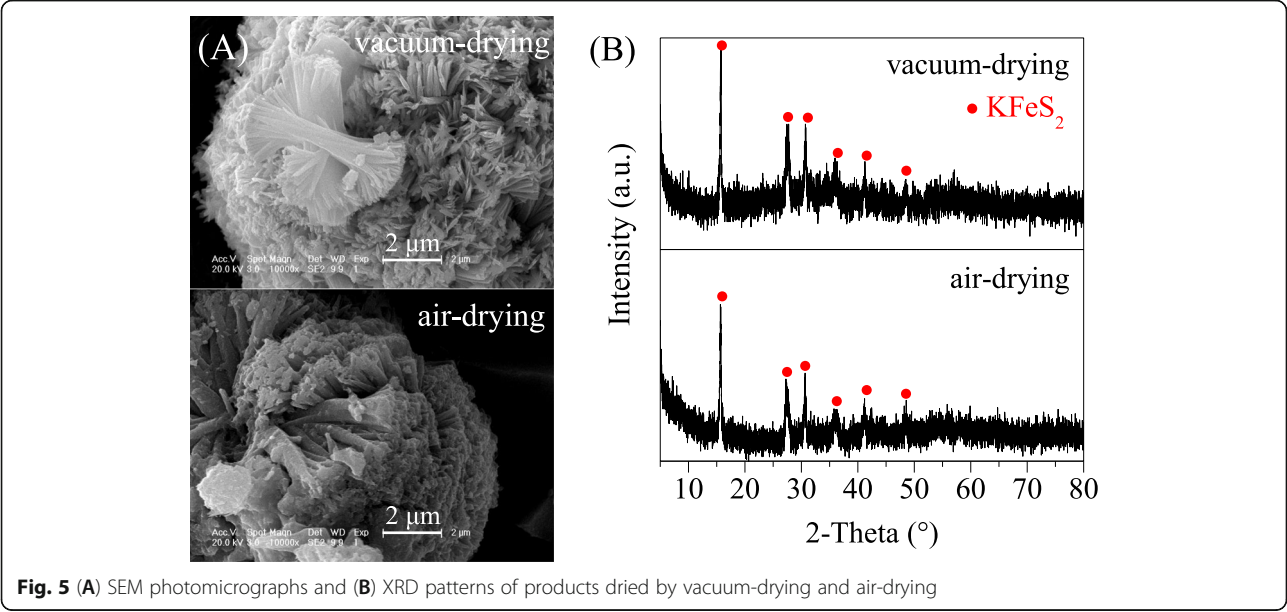

Fig. 4 (**A**) SEM photomicrographs and (**B**) XRD patterns of products synthesised in the repeated experiments

Fig. 5 (**A**) SEM photomicrographs and (**B**) XRD patterns of products dried by vacuum-drying and air-drying

Fig. 6 Treatment of raw electroplating wastewater. (**A**) the dosage effect of P80–24 and corresponding final pH; (**B**) P80–24 compared with the wet P80–24 and other synthesised products; (**C**) P80–24 compared with other reagents (experimental condition: dosage = 1 g L^{-1} (except Fig. 6A) and initial pH = 7.42)

L^{-1} Ni; it was discharged from the electroplating waste-water plant after the addition of precipitant and coagulant. In the effluent, Zn/Ni was at high concentrations, which should be further removed in accordance with the discharge standard of the electroplating industry (electroplating pollutant emission standards [GB21900–2008]). By adding P80–24, Zn/Ni was apparently removed from 0.33 and 0.21 mg L^{-1} with 0.2 g to 0.22 and less than 0.1 mg L^{-1} with 1 g, which could not be detected with 10 g, thereby meeting the concentration of Zn and Ni (1 and 0.5 mg L^{-1}, respectively) in electroplating wastewater discharge standards of China. This result indicated that P80–24 was effective in removing Zn/Ni. The optimal dosage of P80–24 was 1 g, where approximately 97% Zn and 84% Ni were removed, whereas the residual Zn/Ni met the discharge standard of electroplating wastewater (electroplating pollutant emission standards [GB21900–2008]).

P80–24 and the products with recycling supernatant showed similar removal efficiencies of Zn/Ni (Fig. 6B), suggesting that the supernatant was recyclable in the preparation of KFeS$_2$. The removal of Zn/Ni using the products from vacuum drying and air drying was also investigated (Fig. 6B). The residual Zn/Ni levels were 0.15 and 0.076 mg L^{-1} when using the product of vacuum drying and steadily increased to 0.16 and 0.16 mg L^{-1} when using the product of air drying, demonstrating that air drying was not desirable in P80–24 drying. The removal performance of undried P80–24 was also investigated, where it had 55% water content; thus, its dosage was 2.22 g after calculating the optimal dosage of dried P80–24. By adding wet P80–24, the residual Zn/Ni levels were 0.16 and 0.051 mg L^{-1}, which were close to that of dried P80–24; these results revealed that wet P80–24 was efficient in Zn/Ni removal, and freeze drying could be completely omitted. Other common reagents, for example, $Na_2S \cdot 9H_2O$, lime, polymeric ferric sulfuric and

sodium diethyldithiocarbamate, were also used in the removal of Zn/Ni (Fig. 6C), but they did not show desirable removal efficiencies in comparison with P80–24. Thus, P80–24 is an applicable reagent in electroplating wastewater treatment.

After using P80–24, the sharp peaks of KFeS$_2$ disappeared, and only weak peaks of Fe-bearing compound appeared (Fig. 7A). Accordingly, a well-formed whisker was not observed, and only irregular blocks were generated (Fig. 7B), indicating the decomposition of KFeS$_2$ in the effluent. P80–24 was also characterised by X-ray photoelectron spectroscopy before and after use (Fig. 8). For the Fe 2p spectra, a typical peak was recorded at the binding energy of 708.4 eV before use, which belonged to structural Fe in $(FeS_2)_n^{n-}$ [35], but it varied to the binding energy of 710.5 eV after use; this phenomenon was in agreement with the decomposition of KFeS$_2$ and the formation of Fe/S-bearing compound [36]. For S 2p, four peaks at the binding energies of 160.3, 161.2, 163.2 and 167.4 eV were recorded before use, which were affiliated with structural S in the Fe-S bond, S^{2-}, S and sulphate, respectively. However, two peaks disappeared after use because of the decomposition of KFeS$_2$. A new peak at the binding energy of 162.6 eV appeared, along with the peaks of elemental S and sulphate, which demonstrated the formation of the Fe-S-Zn/Ni bond in the decomposed product of KFeS$_2$ after use.

Formation and hydrolysis mechanism of KFeS$_2$

KFeS$_2$ whisker had a one-dimensional linear structure, in which an Fe atom was coordinated with four S atoms. It was stable in alkaline solution at pH > 13.6 and commonly formed in strong alkaline solution. Firstly, when Fe^{3+} was added in the alkaline solution, it was rapidly polymerised to form Fe-bearing precipitates in weakly crystallised form. The sludge acquired from the cold-rolling company showed characteristics similar to the
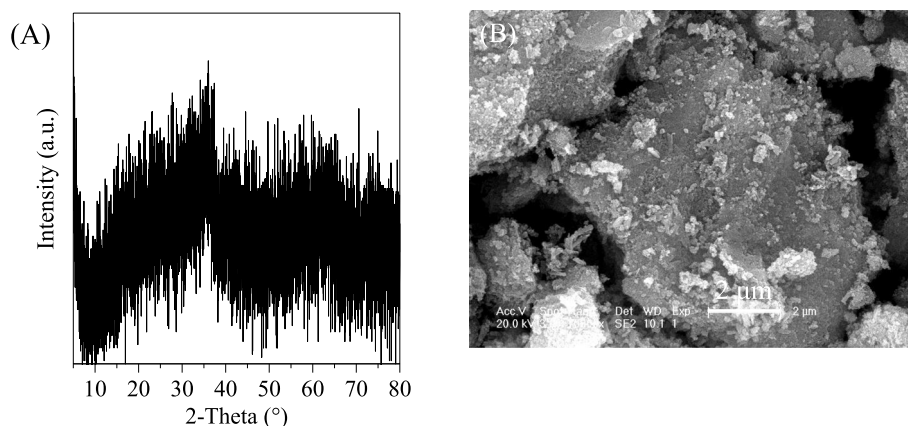

Fig. 7 (**A**) XRD pattern and (**B**) SEM photomicrographs of used PK80–24 after electroplating effluent treatment
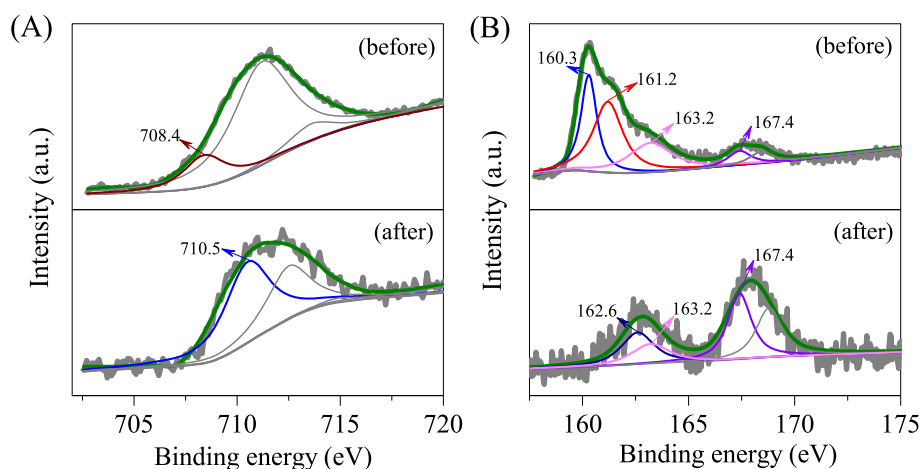
Fig. 8 High-resolution (**A**) Fe 2p and (**B**) S 2p XPS curves of P80–24 before and after use

Fe-bearing precipitates; a small portion of carbon was obtained from the dropped emulsion oil [37]. With the addition of KOH and the hydrolysis of K_2S, free OH^- was abundantly generated in the solution, which eroded the Fe surface of sludge to generate and release $Fe(OH)_4^-$ into the solution. Accordingly, the Fe concentration increased in the supernatant. The concentration of Fe was $0.045 \, mg \, L^{-1}$ at pH 7 (Fig. 9), which rapidly increased to $5.60 \, mg \, L^{-1}$ at pH 15.6, suggesting the dissolution of Fe-bearing precipitates and sludge in strong alkaline solution. Secondly, free SH^- was generated at mass production from the hydrolysis of K_2S, which spontaneously replaced OH^- of free $Fe(OH)_4^-$ to form $Fe(OH)_3HS^-$. The replacement reaction continued, where Fe/S-bearing products, for example, $Fe(OH)_3HS^-$ and $Fe(OH)_2(HS)_2^-$, were generated. Thirdly, the conjunction reaction between two newly formed Fe/S-bearing products occurred to form $(FeS_2) Fe(OH)_3HS^{2-}$. Such products were sparingly soluble in alkaline solution

and precipitated from the solution. The concentration of Fe was residual at $0.184 \, mg \, L^{-1}$ in the supernatant after the reaction (Fig. 9); this residual level was lower than that in pure KOH solution, demonstrating that Fe/S-bearing products were formed and spontaneously precipitated from the solution. The conjunction reaction continued, which accelerated the polymerisation of Fe/S-bearing products, with the generation of linear $(FeS_2)_n^{n-}$ as the final product. Fourthly, in the $(FeS_2)_n^{n-}$ structure, the negative charge was neutralised by free K^+, resulting in the formation of one-dimensional $KFeS_2$ whisker. The related formation process is shown in Fig. 10. However, the reaction of HS^- replaced OH^- of $Fe(OH)_4^-$ to form $Fe(OH)_3HS^-$ was commonly endothermic, which was slow at 50 °C, thereby $KFeS_2$ was not formed even for 24 h.

Some impurities such as Cr, Mn, Si and Al showed some characteristics in the presence of S^{2-} and alkaline solution, which affected the formation of the $(FeS_2)_n^{n-}$
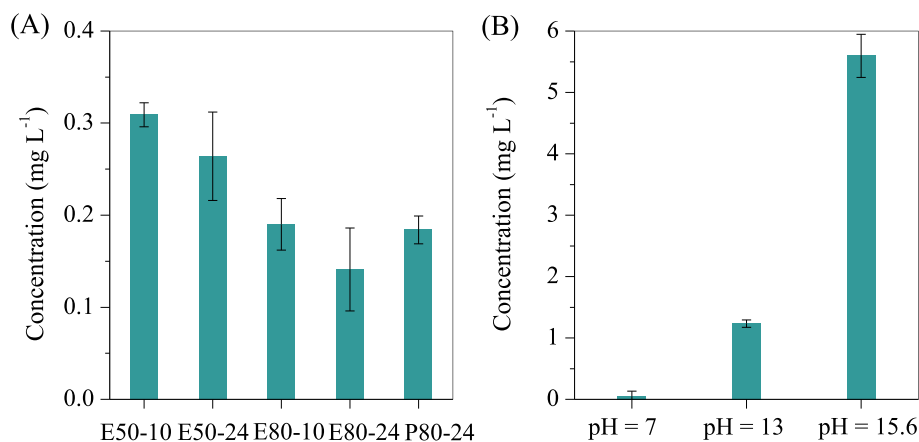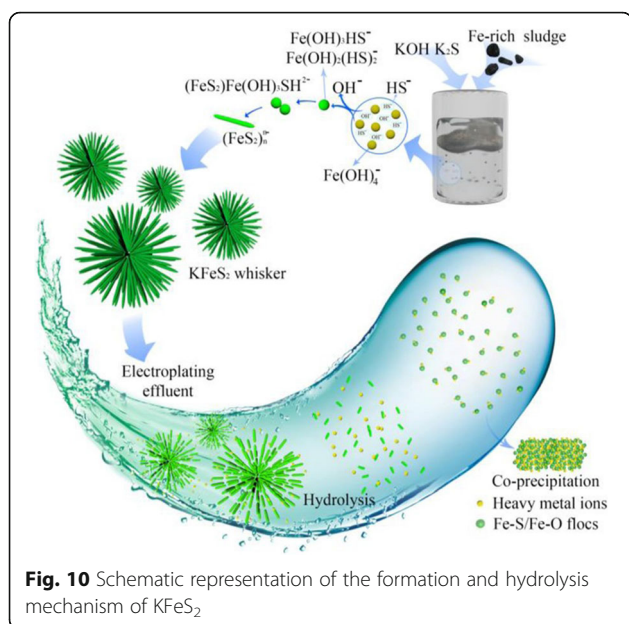

Fig. 9 Fe concentration of the supernatant after (**A**) $KFeS_2$ synthesis and (**B**) alkaline leaching of Fe-bearing sludge

Fig. 10 Schematic representation of the formation and hydrolysis mechanism of KFeS$_2$

group. For instance, when impurities such as Cr and Mn were present in the sludges, the redox reaction between Cr/Mn and S^{2-} occurred, with the generation and release of free OH$^-$ to solution. Therefore, the released OH$^-$ were accumulated in the solution, which promoted the formation of Fe (OH)$_4^-$, polymerisation of the (FeS$_2$)$_n^{n-}$ group and crystallisation growth [27, 38]. Conversely, the impurities of Si/Al-bearing minerals were easily dissolved in the alkaline solution, which not only consumed extra OH$^-$, but also spontaneously polymerised and crystallised new Si/Al-bearing products, such as sodalite and cancrinite. Other elements, for example, Ca and Co, were reacted with S^{2-} to form corresponding sulphide [39]. Such impure elements did not coordinate into the crystal structure of (FeS$_2$)$_n^{n-}$. Here, impure carbon was not involved in KFeS$_2$ synthesis, and it did not accumulate in the supernatant. After the reaction, the supernatant was alkaline and rich in HS$^-$, which could serve as a cyclable resource to prepare KFeS$_2$ with supplementary K$_2$S and KOH. Thus, the dosage of K$_2$S and KOH was considerably reduced. Temperature was an important parameter in KFeS$_2$ synthesis. As the temperature increased from 50 to 80 °C, the reaction between OH$^-$ and the surface Fe of sludge and the release of Fe (OH)$_4^-$ to solution accelerated, which used sufficient Fe (OH)$_4^-$ for the polymerisation and crystallisation of KFeS$_2$ whisker. Accordingly, high temperature was an important route to reduce the reaction time. For instance, linear KFeS$_2$ particles were generated after hydrothermal treatment at 190 °C for 18 h [9]. The drawback of high-temperature treatment in water was the formation of hematite from the rapid

polymerisation of the surface of the Fe-OH group of sludge [9, 40, 41].

Before its application in wastewater treatment, the storage of KFeS$_2$ was a key step. Wet KFeS$_2$ particles remained stable for a week and showed a similar effect to freeze-dried KFeS$_2$ in the removal of heavy metals from effluent. Apart from wet storage, vacuum drying could be used as an alternative method to KFeS$_2$ storage, where the dried product showed a similar effect to freeze drying in Zn/Ni removal. During air drying, the redox reaction between oxygen and structural S of KFeS$_2$ occurred. This phenomenon led to the consumption of KFeS$_2$ and accordingly decreased Zn/Ni removal efficiency in comparison with freeze drying.

In the effluent, heavy metals were complexed with organics to form stable organic-heavy metal ligands; therefore, they were refractory to be removed, although the precipitates (e.g., lime and polymeric ferric sulfuric) were added. When KFeS$_2$ was added in the electroplating effluent, it was spontaneously decomposed to generate Fe/S-bearing flocs with numerous Fe-SH and Fe-OH groups [26]. Such flocs were negatively charged (Fig. 11A), which had an average hydrodynamic radius of 600 nm (Fig. 11B). Subsequently, heavy metals, for example, Zn and Ni, were coordinated onto the Fe-S/Fe-O groups, resulting in the removal of Zn/Ni from effluent (Fig. 10). In comparison with the hydroxyl group, the new -SH group had strong affinity for complex heavy metals because S had a larger atomic radium than O, and it was more electronegative to from the -S-Me group than O [42]. After heavy metal coagulation, the zeta potential of flocs apparently increased from − 50 to − 35 mV, where its radium considerably increased to 3500 nm, demonstrating the polymerisation of flocs in the removal of Zn/Ni. Floc polymerisation continued when stirring was slow and/or stopped, resulting in the generation of heavy metal-bearing sludge.

Environmental application

The conversion of cold-rolling sludge to KFeS$_2$ was performed at pilot scale, and the product KFeS$_2$ whisker showed superior efficiency in the treatment of real electroplating effluent containing Zn/Ni. The total cost of KFeS$_2$ synthesis was calculated (Table 1). In the first round, the conversion of sludge to KFeS$_2$ whisker was performed on the basis of the optimal molar ratio of Fe: K$_2$S: KOH = 1:5:30. This conversion required 3.45 t of K$_2$S, 10.56 t of KOH, 31.5 t of water and 840.5 kWh power, which amounted to USD 7075. After collecting the produced KFeS$_2$ whisker, the remaining supernatant was rich in K$_2$S and KOH, which was recycled completely in the second round. 1.38 t of K$_2$S and 0.34 t of KOH were supplemented to maintain the optimal molar ratio for KFeS$_2$ synthesis, the reagent cost was only USD
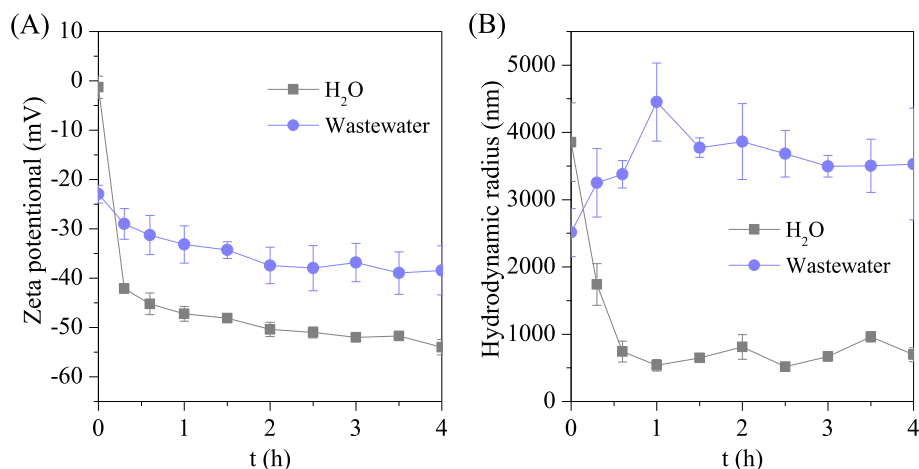
Fig. 11 (**A**) Zeta potential and (**B**) hydrodynamic radius of PK80–24 during its hydrolysis in deionised water and electroplating wastewater

1073, nearly 15% of that in the first round, and the total cost was USD 1254. In addition, the wet $KFeS_2$ showed similar performance to the dried one, suggesting that drying can be omitted, and the wet storage of $KFeS_2$ was also acceptable. This behaviour apparently reduced the total cost in the second round for $KFeS_2$ synthesis. However, about USD 373.3 was spent in the disposal of 1000 kg of sludge [43], and this amount can be deducted from the total cost of $KFeS_2$ synthesis. The $KFeS_2$-bearing product was marketable because of its performance in electroplating wastewater treatment. Therefore, the recycling of cold-rolling sludge as a $KFeS_2$-bearing product was profitable.

Other Fe^{3+}-bearing sludge was also produced as a solid waste in the steel-making, dye chemical and mineral industries; it could function as an Fe^{3+}-bearing resource, which can be recycled as a $KFeS_2$ whisker. Such recycling not only saved the disposal cost of sludge but also

produced new a Fe/S-bearing product, thereby exhibiting acceptable application in these industries.

Conclusions

The conversion of Fe^{3+}-bearing sludge to $KFeS_2$ whisker at low temperature was performed successfully. In the lab-scale experiment, ferrihydrite was used as an Fe resource; after treatment at 80 °C for 24 h, a well-formed $KFeS_2$ whisker was obtained. At pilot scale, the cold-rolling sludge was used as Fe^{3+}-bearing resource, and $KFeS_2$ whisker was also produced at mass production. The generated supernatant was completely recycled by the supplement of K_2S, KOH and tap water for $KFeS_2$ synthesis in the next round. After supernatant cycling for five times, the product was also in the form of $KFeS_2$ whisker. Freeze drying and vacuum drying were desirable methods to dry $KFeS_2$, except air drying. The $KFeS_2$

Table 1 Total cost of the recycling supernatant for $KFeS_2$ synthesis from cold-rolling sludge

	Reagent and processing	Cost	Usage	Subtotal cost (USD t^{-1})
Recycling of used alkaline solution for $KFeS_2$ synthesis	Fe-bearing sludge	0	0.86 t	0
	Supplementary Potassium sulphide	673.3 USD t^{-1}	1.38 t	929.15
	Supplementary Potassium hydroxide	432.5 USD t^{-1}	0.34 t	147.05
	Tap water	0.28 t^{-1}	3.1 t	0.86
	Pulping	0.21 USD/ kWh	0.5 kW (total 1 h)	0.11
	Hydrothermal reaction	0.21 USD/ kWh	30 kW (total 24 h)	151.2
	Drying	0.21 USD/ kWh	6 kW (total 20 h)	25.2
Total cost				1253.57

whisker was effective for treating real electroplating effluent containing Zn and Ni. Moreover, wet $KFeS_2$ and the product obtained from supernatant recycling showed similar removal efficiencies of Zn/Ni to $KFeS_2$ whisker obtained freeze drying, which exhibited a simple and convenient method of storing $KFeS_2$ products.

Supplementary Information

The online version contains supplementary material available at https://doi.org/10.1186/s42834-021-00098-4.

> **Additional file 1.**

Authors' contributions

Dongxu Liang: Writing - Original Draft. Yu Chen: Writing - Review & Editing. Suiyi Zhu: Conceptualization, Resources, Funding acquisition, Project administration. Yidi Gao: Data Curation, Formal analysis. Tong Sun: Investigation, Validation. Kyonghun Ri: Visualization, Validation. Xinfeng Xie: Conceptualization, Supervision. All authors read and approved the final manuscript.

Availability of data and materials

All data generated or analyzed during this study are available from the corresponding author on reasonable request.

Declarations

Competing interests

The authors declare they have no competing interests.

Author details

[1]Science and Technology Innovation Center for Municipal Wastewater Treatment and Water Quality Protection, Northeast Normal University, Changchun 130117, China. [2]Mining Faculty, Kimchaek University of Technology, Pyongyang 999093, North Korea. [3]School of Forest Resources and Environmental Science, Michigan Technological University, Houghton 49931, USA.

References

1. Tiwary SK, Vasudevan S. Single crystal magnetic susceptibility of the quasi-one-dimensional antiferromagnet $KFeS_2$. Solid State Commun. 1997;101:449–52.
2. Osadchii VO, Voronin MV, Baranov AV. Phase equilibria in the $KFeS_2$–Fe–S system at 300–600 °C and bartonite stability. Contrib Mineral Petr. 2018;173:44.
3. Amthauer G, Bente K. Mixed-valent iron in synthetic rasvumite, KFe_2S_3. Naturwissenschaften. 1983;70:146–7.
4. Debiasi RS, Taft CA. Magnetic resonance in $KFeS_2$ single crystals. J Mater Sci. 1978;13:2274–75.
5. Allali N, Favard JF, Rambaud M, Goloub A, Danot M. Low-temperature reactions using potassium iron disulfide as a precursor. Mater Res Bull. 1994;29:135–42.
6. Boller H. Faserförmige Erdalkali-thioferrate [Fibrous alkaline earth thioferrates]. Monatshefte für Chemie. 1978;109:975–85 [in German].
7. Galembeck A, Alves OL. Thermal behavior of α-Ba $(FeS_2)_2$ and $AgFeS_2$: quasi-unidimensional and 3D network compounds prepared from ion-exchange on the same precursor. J Mater Sci. 1999;34:3275–80.
8. Guo JG, Chen XL, Wang G, Jin SF, Zhou TT, Lai XF. Effect of doping on electrical, magnetic, and superconducting properties of $K_xFe_{2-y}S_2$. Phys Rev B. 2012;85:054507.
9. Han I, Jiang ZL, dela Cruz C, Zhang H, Sheng HP, Bhutani A, et al. Accessing magnetic chalcogenides with solvothermal synthesis: $KFeS_2$ and KFe_2S_3. J Solid State Chem. 2018;260:1–6.
10. Guy JK, Spann RE, Martin BR. Solid state ion exchange chemistry of the solid solution $K_xRb_{1-x}FeS_2$. Solid State Ionics. 2008;179:409–14.
11. Arguello Z, Torriani I, Furtado NC, Arsenio TP, Taft CA. The growth of single crystals of $KFeS_2$ and $RbFeS_2$ by the Bridgman method. J Cryst Growth. 1984;67:483–5.
12. Boon JW. The crystal structure of chalcopyrite ($CuFeS_2$) and $AgFeS_2$: the permutoidic reactions $KFeS_2 \rightarrow CuFeS_2$ and $KFeS_2 \rightarrow AgFeS_2$. Recl Trav Chim Pay-B. 1944;63:69–80.
13. Sciacca B, Yalcin AO, Garnett EC. Transformation of Ag nanowires into semiconducting $AgFeS_2$ nanowires. J Am Chem Soc. 2015;137:4340–3.
14. Nsude HE, Nsude KU, Whyte GM, Obodo RM, Iroegbu C, Maaza M, et al. Green synthesis of $CuFeS_2$ nanoparticles using mimosa leaves extract for photocatalysis and supercapacitor applications. J Nanopart Res. 2020;22:352.
15. Kiiamov A, Lysogorskiy Y, Seidov Z, von Nidda HAK, Tsurkan V, Tayurskii D, et al. Vibrational properties and lattice specific heat of $KFeS_2$. AIP Conf Proc. 2018;2041:040002.
16. Ding BB, Yu C, Li CX, Deng XR, Ding JX, Cheng ZY, et al. cis-Platinum pro-drug-attached $CuFeS_2$ nanoplates for *in vivo* photothermal/photoacoustic imaging and chemotherapy/photothermal therapy of cancer. Nanoscale. 2017;9:16937–49.
17. Johnston DC, Mraw SC, Jacobson AJ. Observation of the antiferromagnetic transition in the linear chain compound $KFeS_2$ by magnetic susceptibility and heat capacity measurements. Solid State Commun. 1982;44:255–8.
18. Bronger W, Kyas A, Muller P. The antiferromagnetic structures of $KFeS_2$, $RbFeS_2$, $KFeSe_2$, and $RbFeSe_2$ and the correlation between magnetic moments and crystal field calculations. J Solid State Chem. 1987;70:262–70.
19. Diakonov II, Schott J, Martin F, Harrichourry JC, Escalier J. Iron (III) solubility and speciation in aqueous solutions. Experimental study and modelling: part 1. Hematite solubility from 60 to 300 °C in NaOH-NaCl solutions and thermodynamic properties of Fe $(OH)_4$–(aq). Geochim Cosmochim Ac. 1999;63:2247–61.
20. Yu J, Saada H, Sojic N, Loget G. Photoinduced electrochemiluminescence at nanostructured hematite electrodes. Electrochim Acta. 2021;381:138238.
21. Tadic M, Kopanja L, Panjan M, Lazovic J, Tadic BV, Stanojevic B, et al. Rhombohedron and plate-like hematite (α-Fe_2O_3) nanoparticles: synthesis, structure, morphology, magnetic properties and potential biomedical applications for MRI. Mater Res Bull. 2021;133:111055.
22. Gou XL, Wang GX, Park J, Liu H, Yang J. Monodisperse hematite porous nanospheres: synthesis, characterization, and applications for gas sensors. Nanotechnology. 2008;19:125606.
23. Liang HF, Chen W, Yao YW, Wang ZC, Yang Y. Hydrothermal synthesis, self-assembly and electrochemical performance of α-Fe_2O_3 microspheres for lithium ion batteries. Ceram Int. 2014;40:10283–90.
24. Lu Y, Sun Z, Huo MX. Fabrication of a micellar heteropolyacid with Lewis-Bronsted acid sites and application for the production of 5-hydroxymethylfurfural from saccharides in water. RSC Adv. 2015;5:30869–76.
25. Ruiz-Gomez MA, Rodriguez-Gattorno G, Figueroa-Torres MZ, Obregon S, Tehuacanero-Cuapa S, Aguilar-Franco M. Role of assisting reagents on the synthesis of α-Fe_2O_3 by microwave-assisted hydrothermal reaction. J Mater Sci-Mater El. 2021;32:9551–66.
26. Wang ZH, Liu YW, Qu Z, Su T, Zhu SY, Sun T, et al. In situ conversion of goethite to erdite nanorods to improve the performance of doxycycline hydrochloride adsorption. Colloid Surface A. 2021;614:126132.
27. Liu YW, Khan A, Wang ZH, Chen Y, Zhu SY, Sun T, et al. Upcycling of electroplating sludge to prepare erdite-bearing nanorods for the adsorption of heavy metals from electroplating wastewater effluent. Water-Sui. 2020;12:1027.
28. Belova L, Vialkova E, Glushchenko E, Burdeev V, Parfenov Y. Treatment of electroplating wastewaters. In: E3S Web of Conferences. Blagoveshchensk: EDP Sciences; 2020.
29. Scarazzato T, Panossian Z, Tenorio JAS, Perez-Herranz V, Espinosa DCR. A review of cleaner production in electroplating industries using electrodialysis. J Clean Prod. 2017;168:1590–602.

30. Chen D, Zhang CS, Rong HW, Zhao MH, Gou SY. Treatment of electroplating wastewater using the freezing method. Sep Purif Technol. 2020;234:116043.
31. Andrus ME. A review of metal precipitation chemicals for metal-finishing applications. Met Finish. 2000;98:20–3.
32. Wang H, Wang H, Zhao H, Yan Q. Adsorption and Fenton-like removal of chelated nickel from Zn-Ni alloy electroplating wastewater using activated biochar composite derived from Taihu blue algae. Chem Eng J. 2020;379: 122372.
33. Chen C, Chen AQ, Huang XF, Ju R, Li XC, Wang J, et al. Enhanced ozonation of Cu (II)-organic complexes and simultaneous recovery of aqueous Cu (II) by cathodic reduction. J Clean Prod. 2021;298:126837.
34. Wang Q, Yu JX, Chen XY, Du DT, Wu RR, Qu GZ, et al. Non-thermal plasma oxidation of Cu (II)-EDTA and simultaneous Cu (II) elimination by chemical precipitation. J Environ Manage. 2019;248:109237.
35. Bronold M, Pettenkofer C, Jaegermann W. Surface analysis investigations on the reaction of FeS_2 with alkali metals. Ber Bunsen Phys Chem. 1991;95: 1475–9.
36. Li J, Xu YL, Zhang Y, He C, Li TT. Enhanced redox kinetics of polysulfides by nano-rod FeOOH for ultrastable lithium-sulfur batteries. J Mater Chem A. 2020;8:19544–54.
37. Liu B, Zhang SG, Pan DA, Chang CC. Synthesis and characterization of micaceous iron oxide pigment from oily cold rolling mill sludge. Procedia Environ Sci. 2016;31:653–61.
38. Zhu SY, Liu YW, Huo Y, Chen Y, Qu Z, Yu Y, et al. Addition of MnO_2 in synthesis of nano-rod erdite promoted tetracycline adsorption. Sci Rep-UK. 2019;9:16906.
39. Hu TK, Wang HM, Ning RY, Qiao XL, Liu YW, Dong WQ, et al. Upcycling of Fe-bearing sludge: preparation of erdite-bearing particles for treating pharmaceutical manufacture wastewater. Sci Rep-UK. 2020;10:12999.
40. Zhu SY, Song X, Chen Y, Dong G, Sun T, Yu HB, et al. Upcycling of groundwater treatment sludge to an erdite nanorod as a highly effienct activation agent of peroxymonosulfate for wastewater treatment. Chemosphere. 2020;252:126586.
41. Zhu SY, Lin X, Dong G, Yu Y, Yu HB, Bian DJ, et al. Valorization of manganese-containing groundwater treatment sludge by preparing magnetic adsorbent for Cu (II) adsorption. J Environ Manage. 2019;236:446–54.
42. Chen Y, Li H, Wang ZP, Tao T, Hu C. Photoproducts of tetracycline and oxytetracycline involving self-sensitized oxidation in aqueous solutions: effects of Ca^{2+} and Mg^{2+}. J Environ Sci-China. 2011;23:1634–9.
43. Zhu SY, Li T, Wu YQ, Chen Y, Su T, Ri KH, et al. Effective purification of cold-rolling sludge as iron concentrate powder via a coupled hydrothermal and calcination route: from laboratory-scale to pilot-scale. J Clean Prod. 2020; 276:124274.

Publisher's Note

Springer Nature remains neutral with regard to jurisdictional claims in published maps and institutional affiliations.